Materials and Methods

RNA Sequencing Sample Collection, Library Preparation, and Analysis. WT and *Δdma1* were grown overnight in BHI media before being diluted to the equivalent of OD 0.1 in 10 mL and grown anaerobically for 4 h at 37°C. Four individual overnight and 10-mL culture biological replicates were prepared. Cultures were normalized, and an amount of culture equivalent to an OD_{600} of 4.0 was pelleted for 90s at 8,000 rpm. Pellets were resuspended on ice in 1 mL TRIzol (Invitrogen) with 10 µL of 5 mg/mL glycogen. Samples were flash frozen and stored at −80°C until extraction. Prior to extraction, samples were thawed on ice, then pelleted, and supernatants were treated with chloroform. RNA was extracted from the aqueous phase using the RNeasy minikit (Qiagen, Inc.), and RNA quality was checked by agarose gel electrophoresis and A_{260}/A_{280} measurements. RNA was stored at −80°C with SUPERase-IN RNase inhibitor (Life Technologies) until library preparation.

RNA sequencing prep (RNA-Seq) was performed as previously describe [1]. Briefly, 400ng of total RNA from each sample was used for generating cDNA libraries following our RNAtag-Seq protocol. PCR amplified cDNA libraries were sequenced on an Illumina NextSeq500, obtaining a high-sequencing depth (over 7 million reads per sample). RNA-Seq data was analyzed using our *in-house* developed analysis pipeline *Aerobio*. Raw reads are demultiplexed by 5' and 3' indices, trimmed to 59 base pairs, and quality filtered (96% sequence quality>Q14). Filtered reads are mapped to the corresponding reference genomes using bowtie2 with the --very-sensitive option (-D 20 –R 3 –N 0 –L 20 –i S, 1, 0.50). Mapped reads are aggregated by feature Count and differential expression is calculated with DESeq2 [1]. In each pair-wise differential expression comparison, significant differential expression is filtered based on two criteria: |log2foldchange| > 1 and adjusted p-value (*padj*) <0.05. All differential expression (DE) comparisons are made between the WT and *Δdma1* mutants under the condition mentioned above. The reproducibility of the transcriptomic data was confirmed by an overall high Spearman correlation across biological replicates (R > 0.95). BioProject ID PRJNA994135.

Sample preparation for Proteomic analysis. WT, *Δdas1*, *Δdma1*, and *Δdas1-dma1* were grown overnight anaerobically in 2mL of BHI media prior to being diluted into 50 mL and grown for 20 h. Whole cells, total membranes, and vesicles were collected from each strain. Four individual biological replicates of each fraction were performed for each strain. Samples were lyophilized in preparation for MS analysis.

Lyophilized protein samples were solubilized in 4% SDS, 100mM Tris pH 8.5 by boiling them for 10 min at 95 °C. The protein concentrations were assessed using a bicinchoninic acid protein assay (Thermo Fisher Scientific) and 100µg of each biological replicate prepared for digestion using Micro S-traps (Protifi, USA) according to the manufacturer's instructions. Briefly, samples were reduced with 10mM DTT for 10 mins at 95°C and then alkylated with 40mM IAA in the dark for 1 hour. Samples were acidified to 1.2% phosphoric acid and diluted with seven volumes of S-trap wash buffer (90% methanol, 100mM Tetraethylammonium bromide pH 7.1) before being loaded onto S-traps and washed 3 times with S-trap wash buffer. Samples were then incubated with Trypsin (1:100 protease:protein ratio, in 100mM Tetraethylammonium bromide pH 8.5) overnight at 37°C before being collected by centrifugation with washes of 100mM Tetraethylammonium bromide pH 8.5, followed by 0.2% formic acid followed by 0.2% formic acid / 50% acetonitrile. Samples were then dried down and further cleaned up using homemade C18 Stage 1,2 tips to ensure the removal of any particulate matter.

Reverse phase Liquid chromatography–mass spectrometry. C18 purified digests were re-suspended in Buffer A* (2% acetonitrile, 0.01% trifluoroacetic acid) and separated on a Ultimate 3000 UPLC (Thermo Fisher Scientific) with a two-column chromatography set up composed of a PepMap100 C18 20 mm x 75 µm trap and a PepMap C18 500 mm x 75 µm analytical column (Thermo Fisher Scientific). Digests were loaded on to the trap column at 5 µL/min for 6 minutes with Buffer A (0.1% formic acid, 2% DMSO) then infused into a Orbitrap 480™ at 300 nl/minute via the analytical column. 95-minute runs were undertaken by altering the buffer composition from 2% Buffer B to 28% B over 70 minutes, then from 25% B to 40% B over 4 minutes, then from 40% B to 80% B over 3 minutes. The composition was held at 80% B for 2 minutes, and then dropped to 2% B over 1 minutes before being held at 2% B for another 10 minutes. The Orbitrap 480™ Mass Spectrometer was operated in a data-dependent mode automatically switching between the acquisition of a single Orbitrap MS scan (300-1600 m/z, maximal injection time of 25 ms, an AGC set to a maximum of 300% and a resolution of 120k) every 3 seconds and Orbitrap MS/MS HCD scans of precursors (using a stepped NCE of 28,32,40%,

maximal injection time of 80 ms, an AGC set to a maximum of 300% and a resolution of 30k). Identification and LFQ analysis were accomplished using MaxQuant (v1.6.17.0)3. Data was searched against the *B. thetaiotaomicron* reference proteome (Uniprot: UP000001414) allowing for oxidation on Methionine. The LFQ and "Match Between Run" options were enabled to allow comparison between samples. Maxquant search results were processed using Perseus (version 1.6.0.7) 3 with missing values imputed based on the total observed protein intensities with a range of 0.3 σ and a downshift of 1.8 σ. Statistical analysis was undertaken in Perseus using two-tailed unpaired T-tests between groups.

Data availability. The mass spectrometry proteomics data has been deposited in the Proteome Xchange accession: PXD043360.

MS data analysis. Identification and LFQ analysis were accomplished using Max-Quant (v2.0.2.0) 8 using *Bacteroides thetaiotaomicron* VPI-5482 proteome (Uniprot: UP000001414) allowing for oxidation on Methionine. Prior to MaxQuant analysis dataset acquired on the Fusion Lumos were separated into individual FAIMS fractions using the FAIMS MzXML Generator9. The LFQ and "Match Between Run" options were enabled to allow comparison between samples. The resulting data files were processed using Perseus (v1.4.0.6)10 to filter proteins not observed in at least four biological replicates of a single group. ANOVA and Pearson correlation analyses were performed to compare groups. Predicted localization and topology analysis for proteins identified by MS were performed using UniProt11, PSORT12, SignalP13 and PULDB14.

LC-MS analysis of lipids from TM and OMVs.
WT, Δ*dma1*, and its complemented strain were grown overnight anaerobically in 5mL of BHI media prior to being diluted into 140 mL and grown for 20 h. TMs and OMVs were collected from each strain. Four individual biological replicates of each fraction were performed for each strain. Total lipids were extracted according to Bligh and Dyer chloroform:methanol method [2]. Briefly, 2 volumes of methanol, 1 volume of chloroform, and 0.8 volumes of Milli-Q water were added to 1 volume of PBS-resuspended sample in solvent-resistant glass tubes. Contents were mixed for 2 min by vortexing, and 1 volume of chloroform was added to the mixture. Samples were vortexed for another minute, then centrifugated for 5 min at 4,000 rpm. After centrifugation, the bottom phase (organic) was recovered using a glass Pasteur pipette and stored in solvent-sealed vials at −80°C until lipid analysis by LC-MS.
Untargeted LC/MS analyses were conducted on an Agilent 6550 A QTOF instrument with an Agilent 1290 high-performance liquid chromatograph (HPLC) with an autosampler, operated using Agilent MassHunter software (Santa Clara, CA, USA). Separation of the total lipid extracts was achieved using a Thermo Fisher (Waltham, MA, USA) BETASIL C_{18} column (100 × 2.1 mm, 5 µm) at a flow rate of 300 µL/min at room temperature. The mobile phase contained 5 mM ammonium formate (pH 5.0) both in solvent A, acetonitrile:water (60:40, vol/vol), and solvent B, isopropanol:acetonitrile (90:10, vol/vol). A gradient elution was applied in the following manner: 68% A, 0 to 1.5 min; 68 to 55% A, 1.5 to 4 min; 55 to 48% A, 4 to 5 min; 48 to 42% A, 5 to 8 min; 42 to 34% A, 8 to 11 min; 34 to 30% A, 11 to 14 min; 30 to 25% A, 14 to 18 min; 25 to 3% A, 18 to 23 min; 3 to 0% A, 25 to 30 min; 0% A, 30 to 35 min; 68% A, 35 to 40 min. Both the positive-ion and negative-ion electrospray ionization (ESI) MS scans were acquired in the mass range of 200 to 2,000 Da at a rate of 2 scans/min. High-resolution (R = 100,000 at m/z 400) mass spectrometric analyses of the lipid extracts were also conducted on a Thermo LTQ Orbitrap Velos. Lipids were loop injected into the ESI ion source using a built-in syringe pump which was set to continuously deliver a flow of 20 µL/min methanol with 0.5% NH_4OH. The scanned mass spectra were recalibrated internally with a known mass, namely, 13:0/15:0 PE at m/z 634.4453. Linear ion trap (LIT) multistage MS (MS^n) spectra were obtained for structural identification as described previously [3–5].

Negative staining and analysis by transmission electron microscopy. For quantitative analyses at the ultrastructural level, 200 mesh formvar/carbon-coated copper grids (Ted Pella Inc., Redding CA) were coated with 50µg/ml poly-L-lysine (Sigma, St Louis, MO) for 10 min at 37°C. Excess fluid was removed, and grids were allowed to air dry. Poly-L-lysine coating allowed for even distribution of material across the grid. Bacterial OMVs were fixed with 1% glutaraldehyde (Ted Pella Inc.) and allowed to absorb onto freshly glow discharged poly-L-lysine-coated grids for 10 min. Grids were then washed in dH_2O and stained with 1% aqueous uranyl acetate

(Ted Pella Inc.) for 1 min. Excess liquid was gently wicked off and grids were allowed to air dry. Samples were viewed on a JEOL 1200EX transmission electron microscope (JEOL USA, Peabody, MA) equipped with an AMT 8-megapixel digital camera (Advanced Microscopy Techniques, Woburn, MA). Each OMV sample was processed in triplicate (3 grids). Ten random images were taken at a magnification of 25,000x from various areas of the grid with a total of 90 images for each sample, and the number of OMV in each image was quantified.

References

1. Zhu, Z. *et al.* Entropy of a bacterial stress response is a generalizable predictor for fitness and antibiotic sensitivity. *Nat. Commun.* 1–15 (2020) doi:10.1038/s41467-020-18134-z.
2. Bligh, E. G. & Dyer, W. J. A RAPID METHOD OF TOTAL LIPID EXTRACTION AND PURIFICATION. *Can. J. Biochem. Physiol.* **37**, 911–917 (1959).
3. Hsu, F.-F. Complete structural characterization of ceramides as [M−H]− ions by multiple-stage linear ion trap mass spectrometry. *Lipidomics Funct. Lipid Biol.* **130**, 63–75 (2016).
4. Hsu, F.-F., Turk, J., Zhang, K. & Beverley, S. M. Characterization of inositol phosphorylceramides from Leishmania major by tandem mass spectrometry with electrospray ionization. *J. Am. Soc. Mass Spectrom.* **18**, 1591–1604 (2007).
5. Hsu, F.-F. & Turk, J. Electrospray ionization with low-energy collisionally activated dissociation tandem mass spectrometry of glycerophospholipids: Mechanisms of fragmentation and structural characterization. *LIPIDOMICS Dev. Appl.* **877**, 2673–2695 (2009).

Supplementary Text

Table S1: Strain, Plasmids, and Oligonucleotides

Strains used in this study			
Name	**Strain**	**Features**	**Reference/Source**
Escherichia coli	s17-1λ*pir*	Conjugation donor strain to introduce plasmids into *B. thetaiotaomicron*	Jeffrey I. Gordon Laboratory
Escherichia coli	BL21	Expression and isolation of heterologous proteins	Tracey Raivio Laboratory
Escherichia coli	BL21 pGSTag	Expresses GST under IPTG inducible promoter	This study
Escherichia coli	BL21 pGSTag_Dma1(1:40)	Expresses the N-terminal 40 aa of Dma1 fused to the C-terminus of GST	This study
Escherichia coli	BL21 pET32a-TRXtag	Expresses TRX under IPTG inducible promoter	This study
Escherichia coli	BL21 pET32a-TRXtag_Das1	Expresses Das1 fused to the C-terminus of TRX	This study
B. thetaiotaomicron	VPI-5482	Wild-type strain. Erm^S	Jeffrey I. Gordon Laboratory
B. thetaiotaomicron	VPI-5482 pwwBoINL-Nluc	Expressing *B. ovatus* inulinase fused to Nluc	This study
B. thetaiotaomicron	VPI-5482 Δ*das1*	*das1* (*bt_4720*) deletion mutant	This study
B. thetaiotaomicron	VPI-5482 Δdma1	*dma1* (*bt_4721*) deletion mutant	This study
B. thetaiotaomicron	VPI-5482 Δ*das1-dma1*	*das1* (*bt_4720*)-*dma1* (*bt_4721*) double deletion mutant	This study
B. thetaiotaomicron	VPI-5482 Δ*das2*	*das2* (*bt_1559*) deletion mutant	This study
B. thetaiotaomicron	VPI-5482 Δ*dma2*	*dma2* (*bt_1558*) deletion mutant	This study
B. thetaiotaomicron	VPI-5482 Δ*das2-dma2*	*das2* (*bt_1559*)-*dma2* (*bt_1558*) double deletion mutant	This study
B. thetaiotaomicron	VPI-5482 Δ*das1*	*das1* (*bt_4720*) deletion mutant, complemented	This study
B. thetaiotaomicron	VPI-5482 Δ*dma1* pwwDma1-His	*dma1* (*bt_4721*) deletion mutant, complemented	This study
B. thetaiotaomicron	VPI-5482 Δ*das1-dma1* pwwDas1-Dma1	*das1* (*bt_4720*)-*dma1* (*bt_4721*) double deletion mutant, complemented	This study
B. thetaiotaomicron	VPI-5482 Δ*dma1* pwwFLAG-Dma1-His	*dma1* (*bt_4721*) deletion mutant expressing pwwFLAG-Dma1-His	This study
Plasmids used in this study			
Name	**Resistance**	**Features**	**Reference/Source**
pSAM-Bt	Amp^R,Erm^R	Vector base to perform transposon mutagenesis	Goodman et al., 2009

pSAM-Bt_Tet	Amp^R,Tet^R	pSAM-Bt backbone containing tetracycline resistance cassette	This work
pSIE1	Amp^R,Erm^R,aTc^S	P1T_DP-GH023_*ss-bte1*; P1T_DP-GH023_*ss-bfe1*; P_{BFP1E6}_tetR	Bencivenga-Barry et al., 2020
pSIE1_das1	Amp^R,Erm^R,aTc^S	pSIE1 deletion construct for *B. thetaiotaomicron* VPI-5482 *das1*	This study
pSIE1_dma1	Amp^R,Erm^R,aTc^S	pSIE1 deletion construct for *B. thetaiotaomicron* VPI-5482 *dma1*	This study
pSIE1_das1-dma1	Amp^R,Erm^R,aTc^S	pSIE1 deletion construct for *B. thetaiotaomicron* VPI-5482 *das1*& *dma1*	This study
pSIE1_das2	Amp^R,Erm^R,aTc^S	pSIE1 deletion construct for *B. thetaiotaomicron* VPI-5482 *das2*	This study
pSIE1_dma2	Amp^R,Erm^R,aTc^S	pSIE1 deletion construct for *B. thetaiotaomicron* VPI-5482 *dma2*	This study
pSIE1_das2-dma2	Amp^R,Erm^R,aTc^S	pSIE1 deletion construct for *B. thetaiotaomicron* VPI-5482 *das2* & *dma2*	This study
pSIE1_BT1287	Amp^R,Erm^R,aTc^S	pSIE1 deletion construct for *B. thetaiotaomicron* VPI-5482 BT_1287	This study
pSIE1_nigD1	Amp^R,Erm^R,aTc^S	pSIE1 deletion construct for *B. thetaiotaomicron* VPI-5482 *NigD1* (BT_4005)	This study
pSIE1_nigD2	Amp^R,Erm^R,aTc^S	pSIE1 deletion construct for *B. thetaiotaomicron* VPI-5482 *NigD2* (BT_4719)	This study
pWW3452	Amp^R,Erm^R	AmpR-ermG-RP4/R6K-[P_BfP1E6-RBSlp-LPGFP-tag-Term]-NBU2, AmpR ErmR	Whitaker et al., 2017
pWW3867	Amp^R,Erm^R	AmpR-ermG-RP4/R6K-[P_BT1311-RBSphageGFP-tag-Term]-NBU2, AmpR ErmR	Whitaker et al., 2017
pwwBoINL-Nluc	Amp^R,Erm^R	pWW3867containing Inulinase-Nluc fusion	This study
pwwNLuc	Amp^R,Erm^R	pWW3867containing Nluc	This study
pwwEV	Amp^R,Erm^R	pWW3867 backbone	Whitaker et al., 2017
pwwDas1-His	Amp^R,Erm^R	pWW3867 containing Das1 with C-terminal 6xHis tag	This study
pwwDma1-His	Amp^R,Erm^R	pWW3867 containing Dma1 with C-terminal 10xHis tag	This study
pwwFLAG-Dma1-His	Amp^R,Erm^R	pWW3867 containing Dma1 with an N-terminal 3xFlag tag and a C-terminal 10xHis tag	This study
pwwDas1-Dma1-His	Amp^R,Erm^R	pWW3867 containing Das1 and Dma1 with C-terminal His tags	This study

pGSTag	Amp^R	Expresses GST and is used to create GST fusion proteins	Ron et al. 1992
pET32a-TRXtag	Amp^R	Expresses TRX and is used to create TRX fusion proteins	Bennett et al. 2002

Oligonucleotides used in this study

Name	Sequence	Template	Description
F_Nluc	GTCTTCACACTCGAAGATTTC	pLenti6.2-Nanoluc-ccdB vector	For cloning into pWW3867
R_RpoD_Nluc(6His)	TCGAGCTAATCAGCTAGGATTTAG TGATGATGATGATGATGACCCGCC AGAATGCGTTC	pLenti6.2-Nanoluc-ccdB vector	For cloning into pWW3867
F_BoIN-RpoD	TCCAAATCTGTTTTTAAAGAATGAA GATAAATAAATTCTTAATAAGCGG	*B. ovatus* ATCC 8483 genomic DNA	For cloning into pWW3867
R_BoIN(5F)Nluc	AAATCTTCGAGTGTGAAGACAGAT CCTCCTCCTCCTTTCTTAGCGCTT AGATAATG	*B. ovatus* ATCC 8483 genomic DNA	For cloning into pWW3867
F_pww-NLuc-His linear	GTCTTCACACTCGAAGATTTC	pLenti6.2-Nanoluc-ccdB vector	For cloning into pWW3867
R_pww-NLuc	TCGAGCTAATCAGCTAGGATTTAG TGATGATGATGATGATGACCCGCC AGAATGCG	pLenti6.2-Nanoluc-ccdB vector	For cloning into pWW3867
F_BT4720-Downstream	GCGGCCGCTCTAGAACTAGTCGC CTTCGTCGTTATG	*B. thetaiotaomicron* VPI-5482 genomic DNA	For cloning into pSIE1
R_BT4720-Downstream	TTTCTCTTCCATATCTCTACTTGCT TATACACGTGTTTACC	*B. thetaiotaomicron* VPI-5482 genomic DNA	For cloning into pSIE1
F_BT4720-Upstream	GTAAACACGTGTATAAGCAAGTAG AGATATGGAAGAGAAAGAATTATG	*B. thetaiotaomicron* VPI-5482 genomic DNA	For cloning into pSIE1
R_BT4720-Upstream	GATTAGCATTATGAGGATCCATTG CTGATCATTGGGTATG	*B. thetaiotaomicron* VPI-5482 genomic DNA	For cloning into pSIE1
F_BT4721_Up	GCGGCCGCTCTAGAACTAGTTGG TCAGGATCTCTTTTATTTCTCTTAC CT	*B. thetaiotaomicron* VPI-5482 genomic DNA	For cloning into pSIE1
R_BT4721_Up	ATCTCTACCTATCCGTTATTCATTA TCCATTC	*B. thetaiotaomicron* VPI-5482 genomic DNA	For cloning into pSIE1
F_BT4721_Down	AATAACGGATAGGTAGAGATTAGA ACCCGGTGTTGCTTATTTCTTTGA TGATG	*B. thetaiotaomicron* VPI-5482 genomic DNA	For cloning into pSIE1
R_BT4721_Down	AAGATTAGCATTATGAGGATCCGG TGACGTATGTTTCAGTGTTC	*B. thetaiotaomicron* VPI-5482 genomic DNA	For cloning into pSIE1
R_BT4720/21-Downstream	ATATAGCTCAACTATATTGATTGCT TATACACGTGTTTACC	*B. thetaiotaomicron* VPI-5482 genomic DNA	For cloning into pSIE1
F_BT4721/20-Upstream	GTAAACACGTGTATAAGCAATCAA TATAGTTGAGCTATATATTTTAAAA GC	*B. thetaiotaomicron* VPI-5482 genomic DNA	For cloning into pSIE1
F_BT1558 Downsteam	GCGGCCGCTCTAGAACTAGTCAG GCACAGTGTCATAG	*B. thetaiotaomicron* VPI-5482 genomic DNA	For cloning into pSIE1
R_BT1558 Downstream	CGCTGATGCCGGGATGACTGTCC TTATAAAAATGAAAAAAACACTTAT G	*B. thetaiotaomicron* VPI-5482 genomic DNA	For cloning into pSIE1

F_BT1558 Upstream	TTTTTTCATTTTTATAAGGACAGTC ATCCCGGC	*B. thetaiotaomicron* VPI-5482 genomic DNA	For cloning into pSIE1
R_BT1558 Upstream	GATTAGCATTATGAGGATCCCGTG CTGCAGCTG	*B. thetaiotaomicron* VPI-5482 genomic DNA	For cloning into pSIE1
F_BT1559 Downstream	GCGGCCGCTCTAGAACTAGTGCT TTCAGCGGGATG	*B. thetaiotaomicron* VPI-5482 genomic DNA	For cloning into pSIE1
R_BT1559 Downstream	ACACCCTCTATGCCAAACAATGAA ATAACCGATCTGTTTCG	*B. thetaiotaomicron* VPI-5482 genomic DNA	For cloning into pSIE1
F_BT1559 Upstream	GAAACAGATCGGTTATTTCATTGT TTGGCATAGAGGG	*B. thetaiotaomicron* VPI-5482 genomic DNA	For cloning into pSIE1
R_BT1559 Upstream	GATTAGCATTATGAGGATCCTTGG ATACCCGCAAG	*B. thetaiotaomicron* VPI-5482 genomic DNA	For cloning into pSIE1
F_BT1287_Dwn	GCGGCCGCTCTAGAACTAGTCCG GTCATCCTTTACG	*B. thetaiotaomicron* VPI-5482 genomic DNA	For cloning into pSIE1
R_BT1287_Dwn	TAAATAATTAAACAGTCACCTTTAG TTAAAGTTTTCATACTTGTTAAAC	*B. thetaiotaomicron* VPI-5482 genomic DNA	For cloning into pSIE1
F_BT1287_Up	GTATGAAAACTTTAACTAAAGGTG ACTGTTTAATTATTTACAG	*B. thetaiotaomicron* VPI-5482 genomic DNA	For cloning into pSIE1
R_BT1287_Up	GATTAGCATTATGAGGATCCAGAG GCGAATGCG	*B. thetaiotaomicron* VPI-5482 genomic DNA	For cloning into pSIE1
F_BT4005_Dwn	GCGGCCGCTCTAGAACTAGTTAG GAAATCCTACGGTAG	*B. thetaiotaomicron* VPI-5482 genomic DNA	For cloning into pSIE1
R_BT4005_Dwn	AGTTATTTATAAAAGTTTTGATTTG TTCCTCTCTTTTTAATTC	*B. thetaiotaomicron* VPI-5482 genomic DNA	For cloning into pSIE1
F_BT4005_Up	TTAAAAAGAGAGGAACAAATCAAA ACTTTTATAAATAACTAAACCTAAA C	*B. thetaiotaomicron* VPI-5482 genomic DNA	For cloning into pSIE1
R_BT4005_Up	GATTAGCATTATGAGGATCCACCT GTTCCTCGC	*B. thetaiotaomicron* VPI-5482 genomic DNA	For cloning into pSIE1
F_BT4719_Dwn	GCGGCCGCTCTAGAACTAGTGAA GTGCTGTTTTTGCC	*B. thetaiotaomicron* VPI-5482 genomic DNA	For cloning into pSIE1
R_BT4719_Dwn	AAAAAACATTTTTATAGTATATCTAG TAATTATAGAAACACTC	*B. thetaiotaomicron* VPI-5482 genomic DNA	For cloning into pSIE1
F_BT4719_Up	TGTTTCTATAATTACTAGATATACTA TAAAAATGTTTTTTAATGAGTACTA TTTAC	*B. thetaiotaomicron* VPI-5482 genomic DNA	For cloning into pSIE1
R_BT4719_Up	GATTAGCATTATGAGGATCCTCTTT CTCTTCCATATCTCTAC	*B. thetaiotaomicron* VPI-5482 genomic DNA	For cloning into pSIE1
F_RpoD_BT4720-His	TCCAAATCTGTTTTTAAAGAATGG AAGAATTTGAGTTGTCG	*B. thetaiotaomicron* VPI-5482 genomic DNA	For cloning into pWW3867
R_RpoD_BT4720-His	TCGAGCTAATCAGCTAGGATCTAG TGATGATGATGATGATGACCTCCG TTATTCATTATCCATTCTTTTAC	*B. thetaiotaomicron* VPI-5482 genomic DNA	For cloning into pWW3867
F_pwwRpoD_BT4721-His	CCAAATCTGTTTTTAAAGAATGGA AGAGAAAGAATTATGG	*B. thetaiotaomicron* VPI-5482 genomic DNA	For cloning into pWW3867
R_pwwRpoD_BT4721-His	TCGAGCTAATCAGCTAGGATCTAA TGATGATGATGGTGATGATGATGA TGATGACCATAAGTAAGTCGGATA CC	*B. thetaiotaomicron* VPI-5482 genomic DNA	For cloning into pWW3867
R_RpoD_BT4720/21-His	TTTCTCTTCCATATCTCTACCTAGT GATGATGATGATGATGACCTCCGT TATTCATTATCCATTCTTTTAC	*B. thetaiotaomicron* VPI-5482 genomic DNA	For cloning into pWW3867
F_pwwRpoD_BT4721/20-His	CATCATCACTAGGTAGAGATATGG AAGAGAAAGAATTATGG	*B. thetaiotaomicron* VPI-5482 genomic DNA	For cloning into pWW3867
F_FLAG-4721_lin	ATGGATTACAAGGACGATG	pWW3452 DNA	For cloning into pWW3452

R_N-term_3x-FLAG_BT4721	ATCCATAATTCTTTCTCTTCTCCAGATTTATCATCATCG	pWW3452 DNA	For cloning into pWW3452
F_Phg_FLAG-BT4721-His	ACGATGATGATAAATCTGGAGAAGAGAAAGAATTATGGATG	*B. thetaiotaomicron* VPI-5482 genomic DNA	For cloning into pWW3452
R_pwwRpoD_BT4721-His	TCGAGCTAATCAGCTAGGATCTAATGATGATGATGGTGATGATGATGATGACCATAAGTAAGTCGGATACC	*B. thetaiotaomicron* VPI-5482 genomic DNA	For cloning into pWW3452
F_pGSTag_lin	GCAGAACGTCGCGAA	pGSTag DNA	For cloning into pGSTag
R_pGSTag_lin	AGATCCACGCGGAAC	pGSTag DNA	For cloning into pGSTag
F_GST-BT4721_1-80aa	ATCTGGTTCCGCGTGGATCTATGGAAGAGAAAGAATTATGG	*B. thetaiotaomicron* VPI-5482 genomic DNA	For cloning into pGSTag
R_GST-BT4721_1-40aa	AGAATTTCGCGACGTTCTGCCTACCTCTCCACAGG	*B. thetaiotaomicron* VPI-5482 genomic DNA	For cloning into pGSTag
F_pET32a-TRX_lin	CATCATCATCATCATCATTGAG	pET32a-TRXtag	For cloning into pET32a-TRXtag
R_pET32a-TRX_lin	CTTGTCGTCGTCGTC	pET32a-TRXtag	For cloning into pET32a-TRXtag
F_TRX-BT4720_His	GTACCGACGACGACGACAAGATGGAAGAATTTGAGTTGTC	*B. thetaiotaomicron* VPI-5482 genomic DNA	For cloning into pET32a-TRXtag
R_TRX-BT4720-His	CAATGATGATGATGATGATGTCCGTTATTCATTATCCATTC	*B. thetaiotaomicron* VPI-5482 genomic DNA	For cloning into pET32a-TRXtag

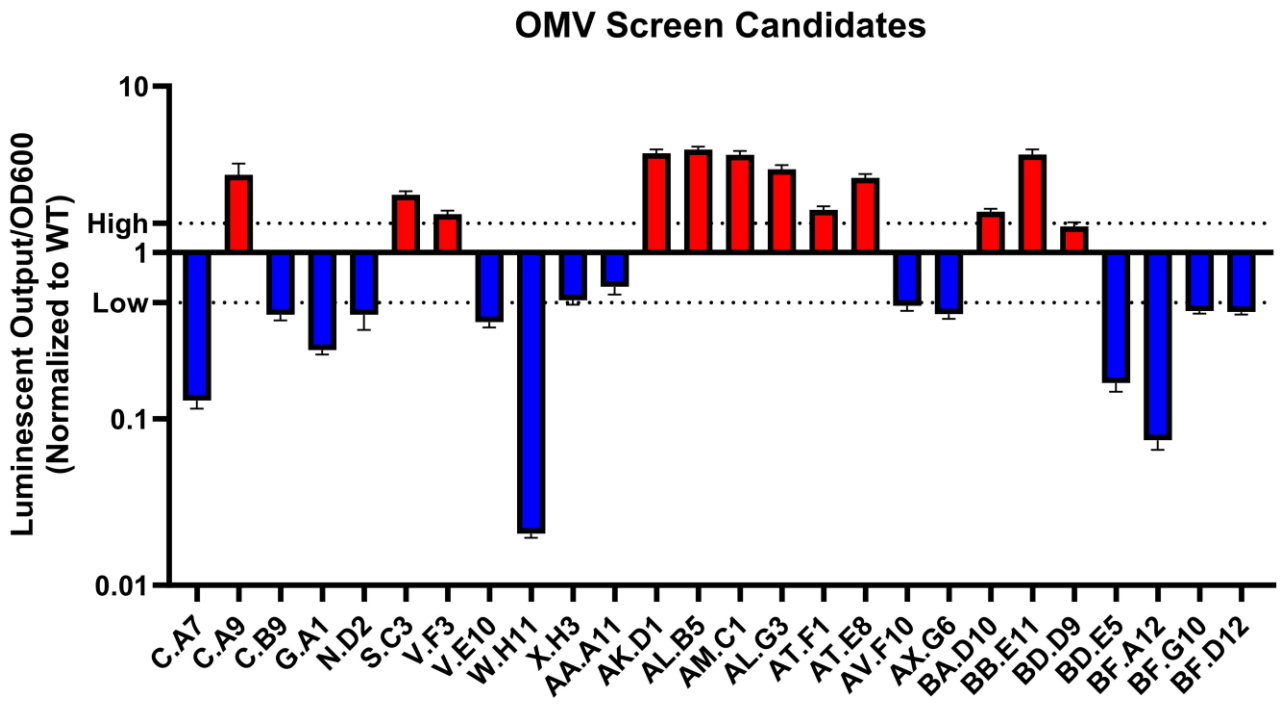

Figure S1: Hyper- and hypovesiculating strains were identified during OMV screening. Nano-Glo assays were performed using filtered supernatants isolated from each potential candidate. Total luminescent output of each candidate was standardized by OD_{600}, then normalized to the wild-type. Candidates exhibiting a 1.5-fold increase in luminescence were considered hypervesiculating, while those displaying a 0.5-fold decrease were deemed hypovesiculating.

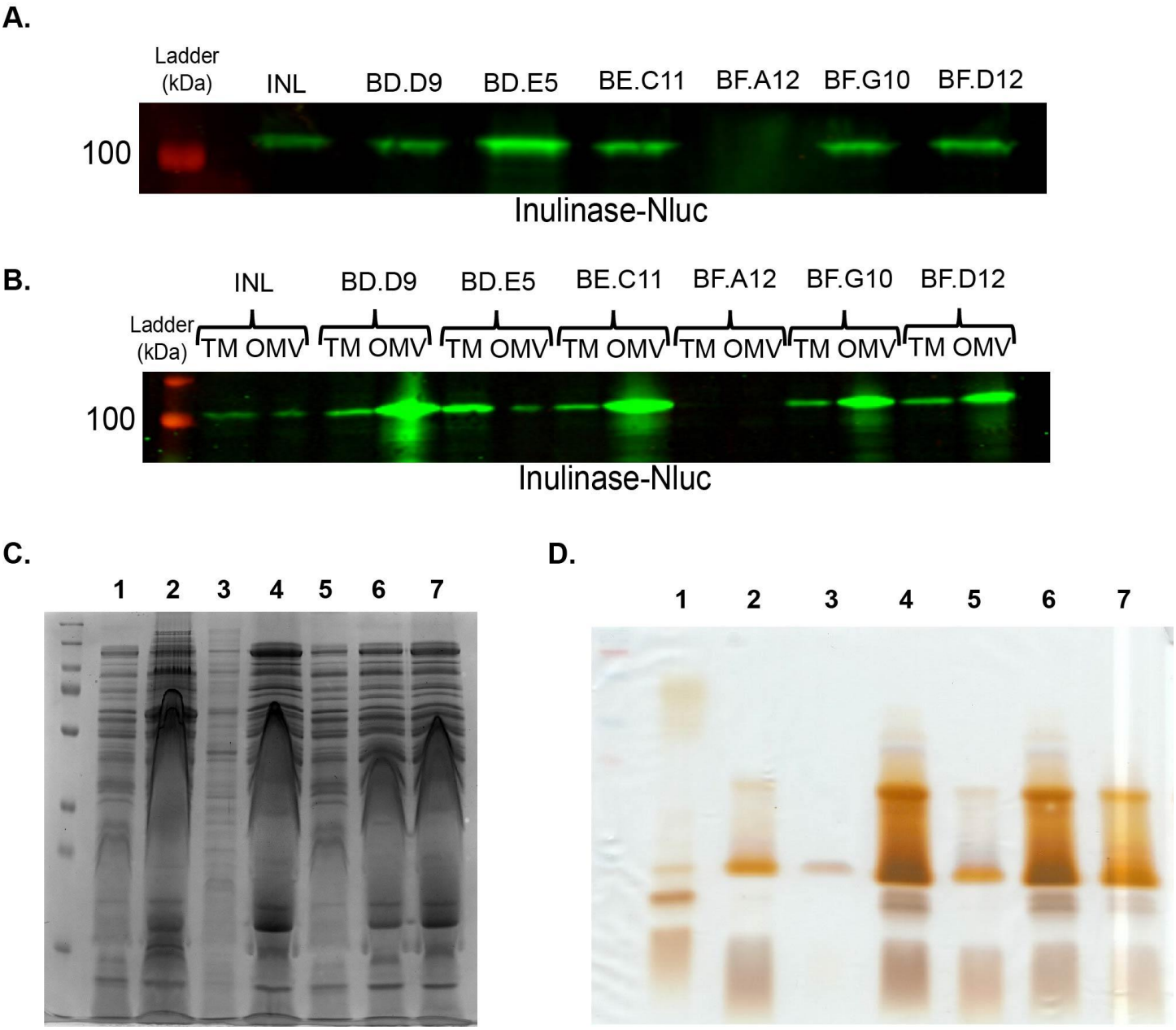

Figure S2: Example of validation for OMV screen candidates. Western blots were performed using (A) whole cells (WCs) to check the expression of the OMV reporter, and (B) TMs and OMVs were isolated to check partitioning of the OMV reporter. (C) Protein profiles of OMVs from each transposon mutant were analyzed by SDS-PAGE followed by Coomassie staining. 1: WT, 2: BD.D9, 3: BD.E5, 4: BE.C11, 5: BF.A12, 6: BF.G10, 7: BF.D12. (D) Relative abundance of LPS content of transposon mutants were analyzed by SDS-PAGE followed by LPS silver staining. 1: *E. coli* 0111:B4, 2: WT, 3: BD.E5, 4: BE.C11, 5: BF.A12, 6: BF.G10, 7: BF.D12

Candidate	Insertion Site(s)	Gene(s) Interrupted	Gene Annotations
C.A7	935,471	BT_0753	Anti-sigma factor
C.A9	458,218; 1,402,418	BT_0372; BT_1115	Aldose 1-epimerase; Aldo/keto reductase
C.B9	4,377,534	BT_3397	Pyruvate ferredoxin oxidoreductase
G.A1	6,138,309	N/A	Insertion in INL-Nluc expression vector
N.D2	2,722,830	N/A	Insertion in intergene region between BT_2164-65
S.C3	3,456,177	BT_2786	30S ribosomal protein s15
V.E10	4,545,446; 5,611,550	BT_3519; BT_4261	SusC-like protein; DUF4847 domain-containing protein
V.F3	2,803,639	BT_2235	Hypothetical protein
W.H11	6,138,327	N/A	Insertion in INL-Nluc expression vector
X.H3	5,611,256	BT_4261	DUF4847 domain-containing protein
AA.A11	4,410,790; 4,545,446	BT_3422; BT_3519	alpha-2-macroglobulin; SusC-like protein
AK.D1	3,115,604	BT_2493	ROK family protein
AL.B5	3,115,511	BT_2493	ROK family protein
AL.G3	N/A	N/A	
AM.C1	3,116,101	BT_2493	ROK family protein
AT.E8	N/A	N/A	
AT.F1	4,820,482	BT_3709	Elongation Factor P
AT.F10	4,820,482	BT_3709	Elongation Factor P
AX.G6	6,196,151	BT_4721	Outer membrane beta-barrel domain-containing protein
BA.D10	4,820,482	BT_3709	Elongation Factor P
BB.E11	3,115,663	BT_2493	ROK family protein
BD.D9	374,098; 4,155,947	BT_0311; BT_3255	2-oxo acid dehydrogenase; N6-adenine-specific DNA methylase
BD.E5	4,304,745	BT_3341	SbsA Ig-like domain-containing protein
BE.C11	6,196,148	BT_4721	Outer membrane beta-barrel domain-containing protein
BF.A12	6,138,331	N/A	Insertion in INL-Nluc expression vector
BF.D12	6,196,613	BT_4721	Outer membrane beta-barrel domain-containing protein
BF.G10	6,196,617	BT_4721	Outer membrane beta-barrel domain-containing protein

Table S2: List of candidate genes identified during OMV Screen.

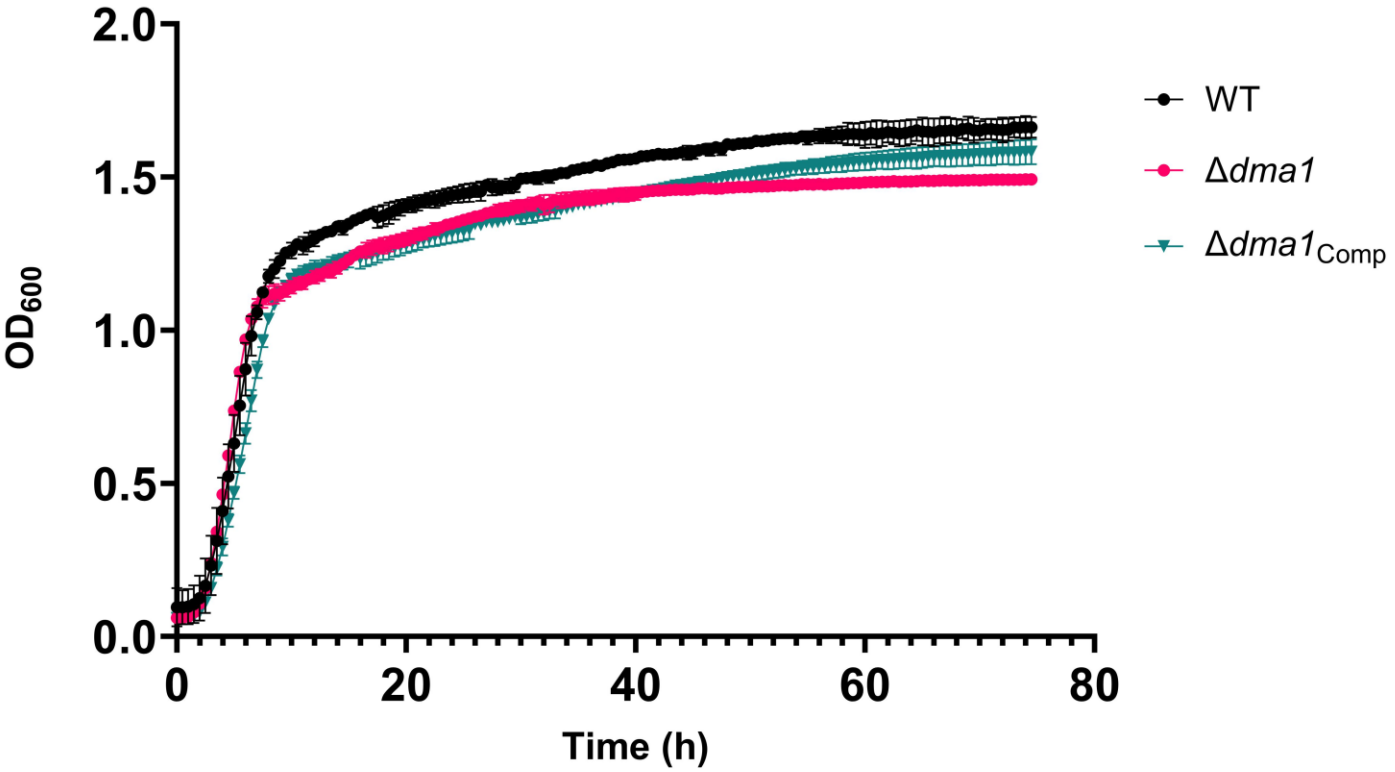

Figure S3: Mutation of *dma1* does not significantly impact growth *in vitro*. Growth curves performed in BHI media for WT, Δ*dma1,* and its corresponding complemented strain.

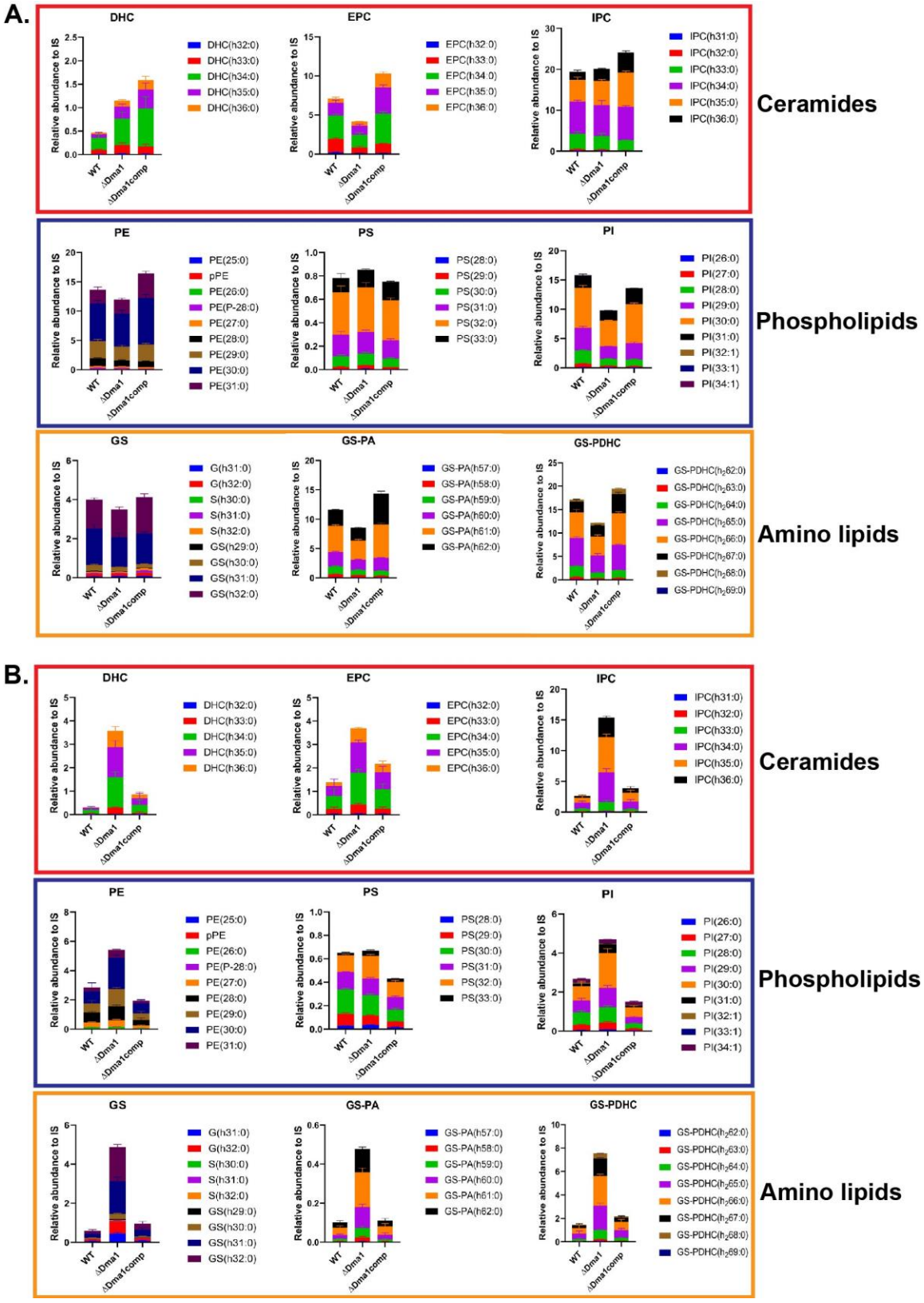

Figure S4: Hypervesiculation causes Δ*dma1* to secrete significantly more membrane lipids. Total lipids were isolated from (A) TM and (B) OMV fractions from WT, Δ*dma1*, and Δ*dma1*$_{Comp}$. Lipids were relativized to an 18:0-20:4 phosphoinositol internal standard (IS). Red squares denote sphingolipids, dihydroceramides (DHC), ethanolamine-phosphoceramides (EPC), inositolphosphoceramide (IPC). Blue squares are phospholipids, phosphatidylethanolamine (PE), phosphatidylserine (PS), and phosphatidylinositol (PI). Yellow square represent amino lipids, glycylserine dipeptide lipids (GS), glycylserine phosphoryl diacylglycerol (GS-PA), N-(3-O-Acyl)acyl glycylserine phosphoryl dihydroceramide (GS-PDHC).

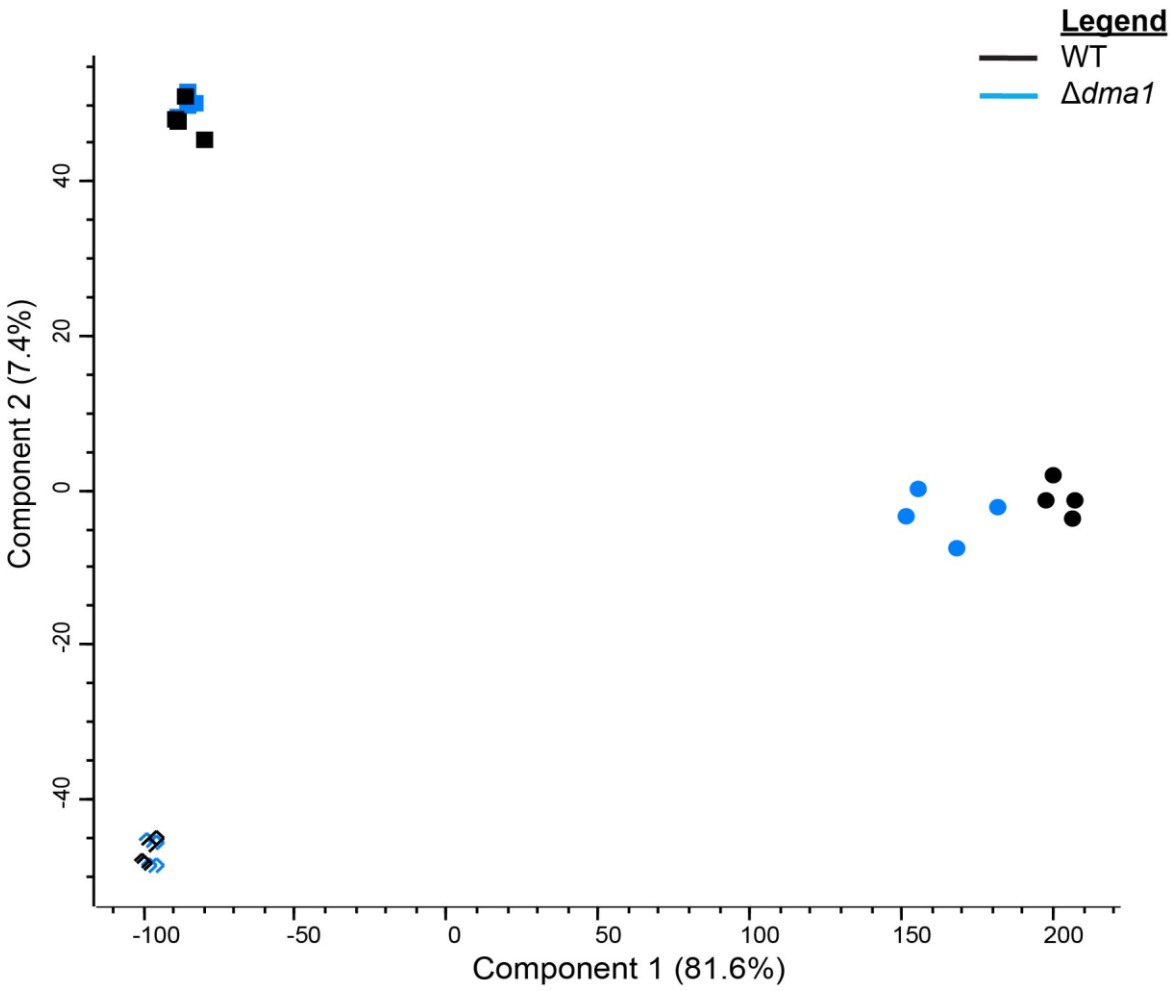

Figure S5: Protein composition of subcellular fractions is consistent between the WT and *Δdma1*. Principal component analysis (PCA) of WC (stars), TM (squares), and OMV (circles) proteomes from *Bt* grown in BHI media. Four biological replicates were performed for each condition.

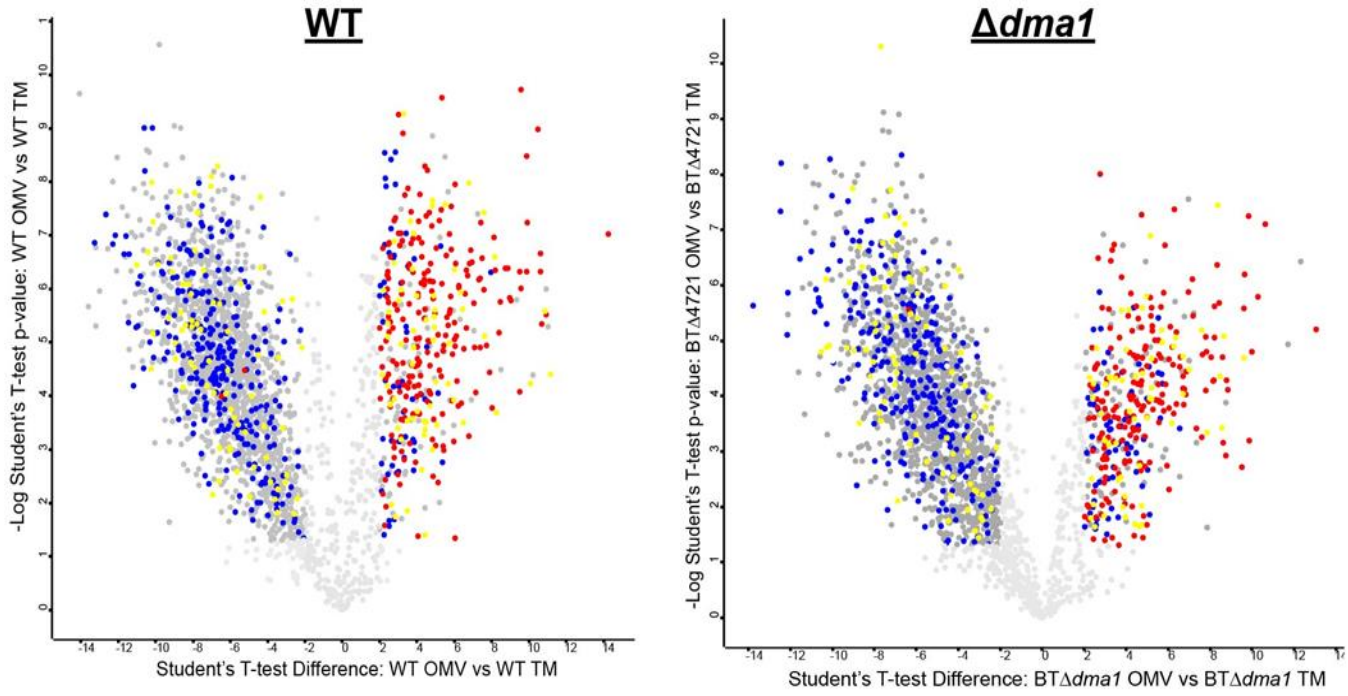

Figure S6: OMV cargo selection is not impacted by mutation of Dma1. Volcano plot representations of proteins enriched in the TM and OMV fractions. Integral membrane proteins are represented in blue, lipoproteins with LES motifs are indicated in red, lipoproteins lacking the LES motif are depicted in yellow, and soluble proteins are indicated in dark gray. (A) OMV cargo selection is maintained in Δ*dma1*, indicating that these OMVs are not the result of cell lysis.

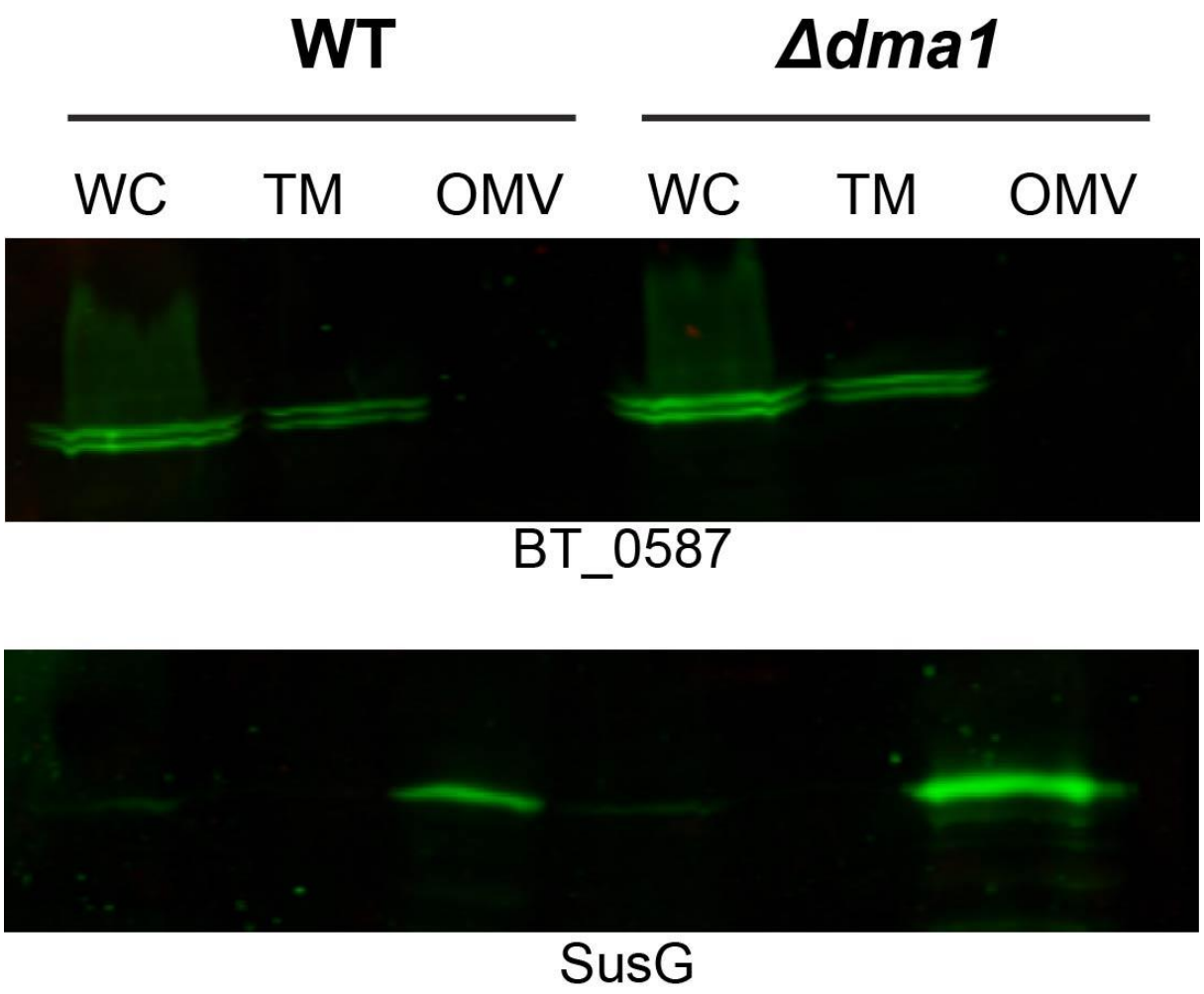

Figure S7: Partitioning of OMV cargo is maintained in *Δdma1*. Western blots using anti-polyHis against different membrane and OMV enriched proteins (*Top*: BT_0587, *Bottom*: SusG (BT_3698)). These demonstrate that partitioning of proteins between the OM and OMVs is not aberrant in *Δdma1*.

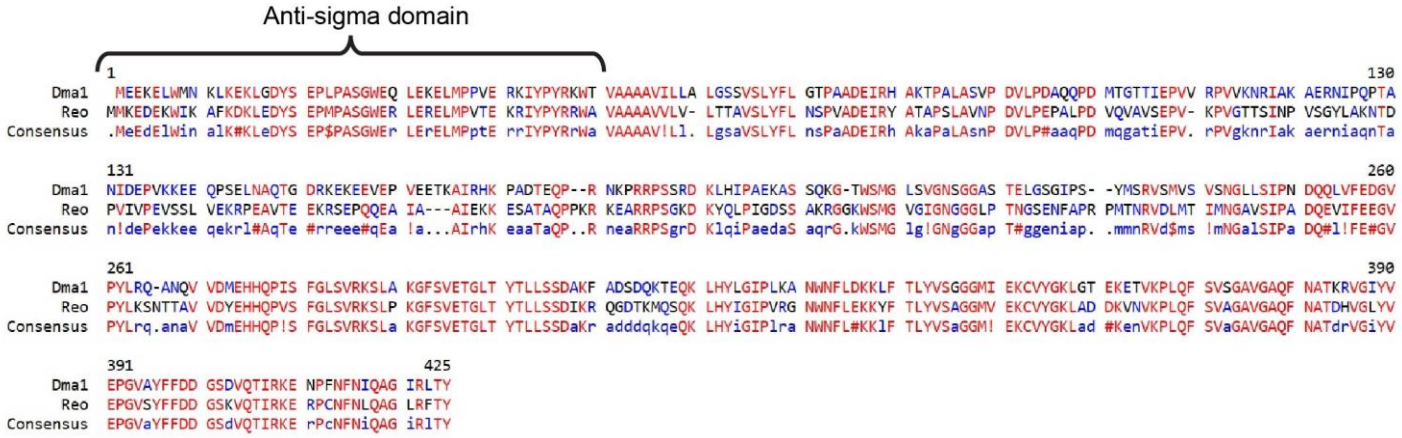

Figure S8: Amino acid sequence alignment of Dma1 and *Bf* Reo. Dma1 show 56% sequence identity with Reo. Amino acids highlighted in red represent high consensus levels (90%), while those in blue represent low consensus (50%). The predicted anti-sigma domain is shown in brackets. Alignment was done using MultAlin version 5.4.1.

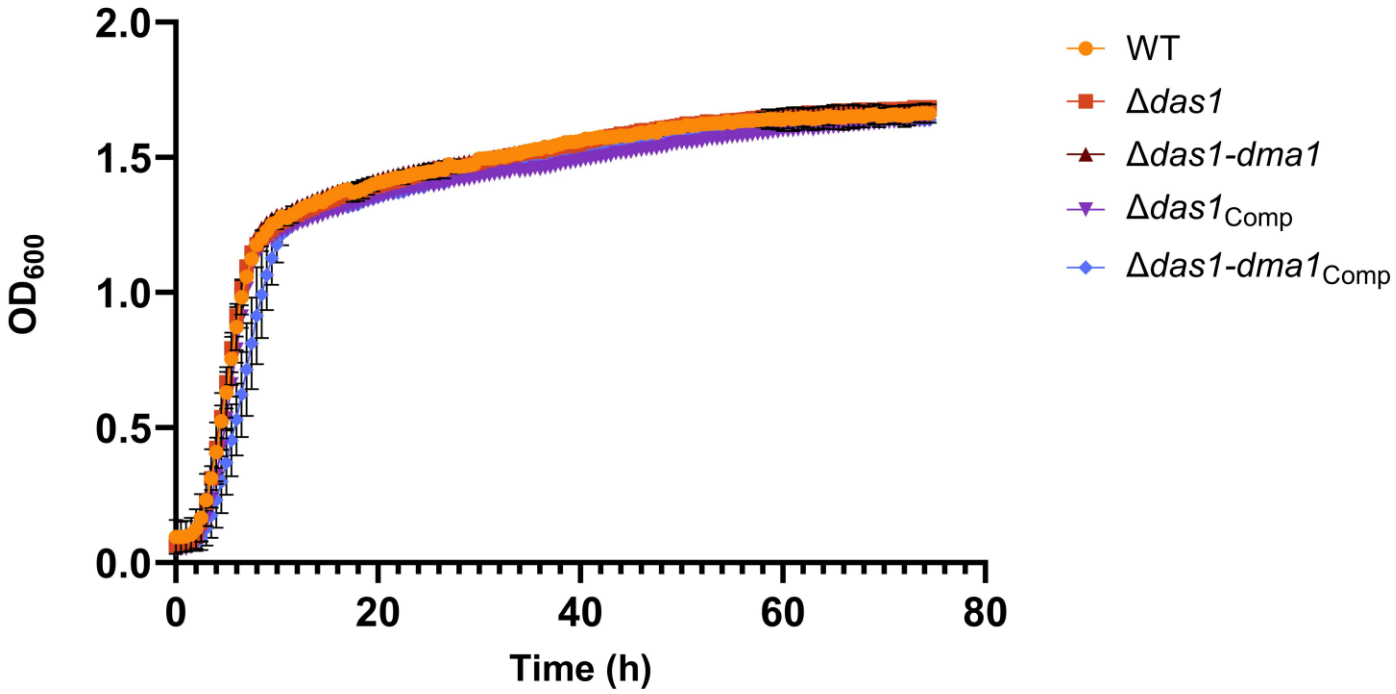

Figure S9: Mutation of *das1* does not impact growth in the wild-type or Δ*dma1* background *in vitro*. Growth curves performed in BHI media for WT, Δ*das1,* Δ*das1-dma1* and their corresponding complemented strain.

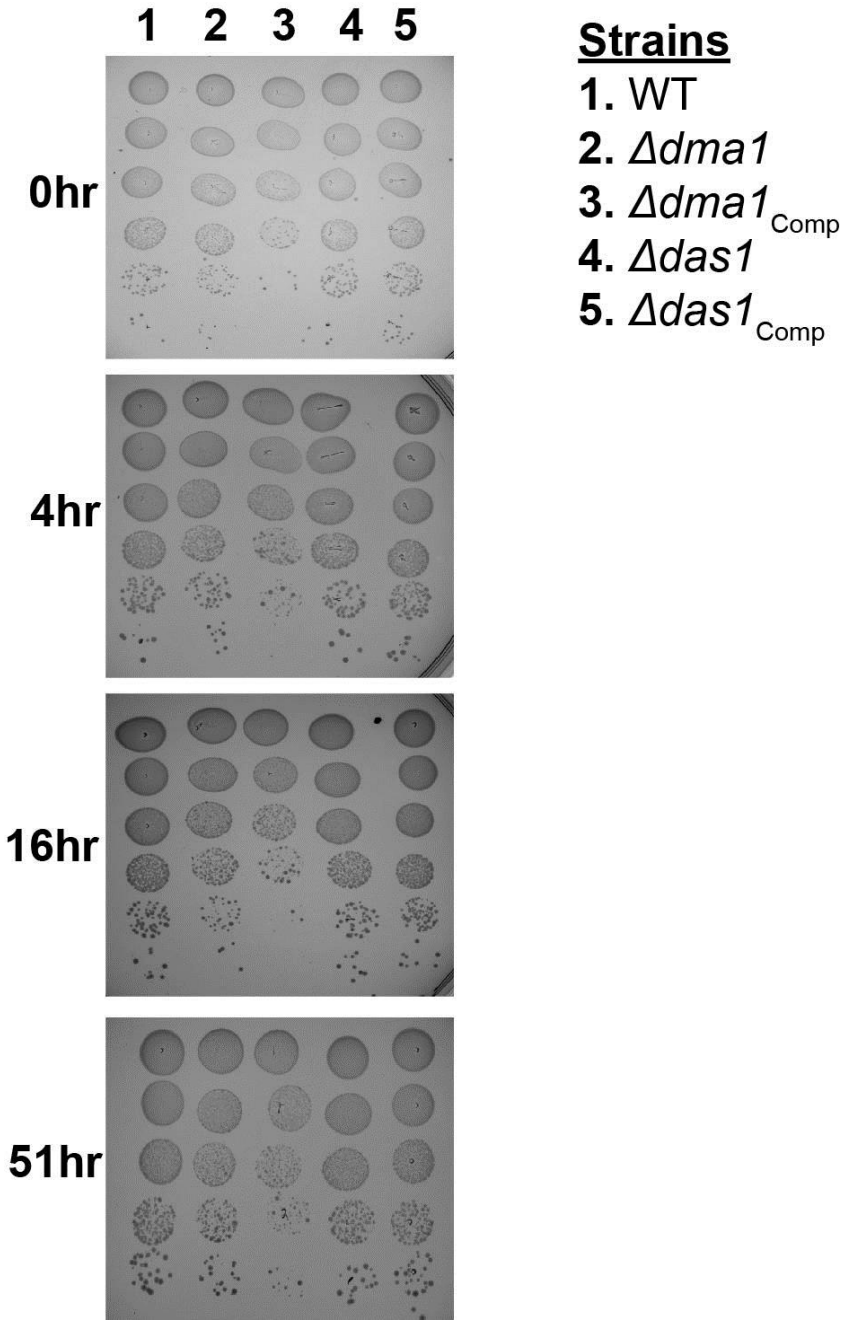

Figure S10: Mutants in Δ*das1* and Δ*dma1* are not attenuated in aerobic stress. Aerobic exposure stress tests comparing WT, Δ*das1*, Δ*dma1*, and their corresponding complemented strains incubated in air for different times. Strains were cultured overnight, then diluted to the equivalent of OD_{600}=0.1 for the initial spot. Each subsequent spot is a ten-fold dilution of the previous one.

Table S3: RNA Sequencing- Δ*dma1* Top 25 Most Upregulated Genes

Gene (New Locus Tag)	Gene (Old Locus Tag)	Log_2FC	Padj	Proposed Function
BT_RS06495	BT_1287	9.879633157	7.34E-26	DUF4840 domain-containing protein
BT_RS20210	BT_4005	7.986054337	2.34E-150	NigD-like protein
BT_RS23775	BT_4719	7.743518851	1.26E-209	NigD-like protein
BT_RS16205	NO	5.229630823	3.24E-05	Smalltalk protein
BT_RS23780	BT_4720	5.034076276	0	Sigma-70 family RNA polymerase sigma factor
BT_RS19750	BT_3913	4.044393237	1.72E-210	DUF5034 domain-containing protein
BT_RS00870	BT_0177	3.767930416	6.95E-285	NigD-like protein
BT_RS00875	BT_0178	3.662030315	0	YIP1 family protein
BT_RS19755	BT_3914	3.590716188	3.32E-192	Hypothetical protein
BT_RS11715	BT_2315	3.579969558	0.0040536	Hypothetical protein
BT_RS24670	NO	3.287601612	0.02828646	Hypothetical protein
BT_RS05220	BT_1038	3.178373436	2.30E-21	endo-beta-N-acetylglucosaminidase family protein
BT_RS20385	BT_4039	3.177706063	1.72E-85	TonB-dependent receptor
BT_RS23805	BT_4725	2.955721786	0.00240863	RagB/SusD family nutrient uptake outer membrane protein
BT_RS05230	BT_1040	2.931638602	1.49E-67	SusC/RagA family TonB-linked outer membrane protein
BT_RS22810	BT_4523	2.926352615	7.39E-155	Type I restriction endonuclease EcoR124II
BT_RS14080	BT_2779	2.860410832	2.41E-68	Class I SAM-dependent methyltransferase
BT_RS10570	BT_2086	2.691908858	1.37E-157	Linear amide C-N hydrolase
BT_RS05210	BT_1036	2.653696133	4.33E-42	DUF1735 domain-containing protein
BT_RS22805	BT_4522	2.637320216	1.54E-52	Type I restriction endonuclease
BT_RS05225	BT_1039	2.5531964	1.13E-38	SusD/RagB family nutrient-binding outer membrane lipoprotein
BT_RS22645	BT_4490	2.541660806	1.52E-17	DUF5025 domain-containing protein
BT_RS05215	BT_1037	2.524779245	1.45E-28	DUF1735 and LamG domain-containing protein
BT_RS12945	BT_2560	2.50963332	8.48E-58	TonB-dependent receptor
BT_RS14845	NO	2.460763495	9.28E-08	Smalltalk protein

Table S3: RNA Sequencing- Δ*dma1* Top 25 Most Downregulated Genes

Gene (New Locus Tag)	Gene (Old Locus Tag)	Log_2FC	Padj	Proposed Function
BT_RS22800	BT_4521	-3.0243084	5.47E-67	Tyrosine-type recombinase/integrase
BT_RS15310	BT_3017	-2.497832498	0.01664662	Acid phosphatase
BT_RS21860	BT_4330	-2.326456539	5.53E-127	Nucleoside permease
BT_RS09755	BT_1926	-2.295427189	5.78E-30	OmpA/MotB domain protein
BT_RS18675	BT_3704	-2.184786525	3.07E-33	Glycoside hydrolase family 13 protein
BT_RS04750	BT_0943	-2.127262731	2.26E-53	Penicillin-binding protein 2B (PBP-2B)
BT_RS13245	BT_2619	-2.123420723	1.05E-74	Histidine kinase
BT_RS21840	BT_4326	-2.112073399	4.79E-98	ATP-binding cassette domain-containing protein
BT_RS16435	BT_3244	-2.081737712	3.53E-50	BACON domain-containing protein
BT_RS04760	BT_0945	-2.078233418	3.80E-50	Hypothetical protein
BT_RS14350	BT_2830	-2.060239218	2.68E-70	HU family DNA-binding protein
BT_RS09760	BT_1927	-1.993238565	3.54E-41	Hypothetical protein
BT_RS16430	BT_3243	-1.909968855	4.73E-51	DUF4302 domain-containing protein
BT_RS13240	BT_2618	-1.881918801	9.75E-09	Two-component system response regulator
BT_RS20375	BT_4037	-1.872169035	1.38E-24	Hypothetical protein
BT_RS15060	BT_2972	-1.835815403	2.91E-23	Class I SAM-dependent methyltransferase
BT_RS10930	BT_2159	-1.822844005	2.25E-148	Gfo/Idh/MocA family oxidoreductase
BT_RS21835	BT_4325	-1.809901243	8.80E-74	ABC transporter permease
BT_RS08875	BT_1751	-1.805310189	2.07E-07	Glycine betaine/L-proline ABC transporter ATP-binding protein
BT_RS21845	BT_4327	-1.801115206	2.77E-108	DUF4836 family protein
BT_RS13230	BT_2615	-1.793091582	1.50E-07	Group II intron reverse transcriptase/maturase
BT_RS04755	BT_0944	-1.791690553	3.24E-11	Hypothetical protein
BT_RS13260	BT_2622	-1.780022703	5.06E-84	Alpha-glucuronidase
BT_RS21850	BT_4328	-1.774306654	1.52E-76	16S rRNA (uracil(1498)-N(3))-methyltransferase
BT_RS10860	BT_2145	-1.764647845	2.52E-85	Adenosylcobalamin-dependent ribonucleoside-diphosphate reductase

Table S4: Comparative Proteomics- Δ*dma1* Top 25 Most Upregulated Genes

Protein ID	Gene	Fold Change	-Log(P-value)	Proposed Function
Q8A887	BT_1287	9.30394	4.16088	DUF4840 domain-containing protein
Q89YL2	BT_4719	6.68855	2.84572	NigD-like protein
Q8A0L6	BT_4005	5.17626	3.95591	NigD-like protein
Q89YS2	BT_4659	3.50177	2.6692	SusD homolog
Q8AB86	BT_0224	3.42438	1.96457	Lipocalin-like protein
Q8ABW9	BT_p548229	3.19438	5.8735	Fimbrillin family protein
Q8A2W6	BT_3189	3.012	1.91681	Unknown
Q8ABX1	BT_p548227	2.75674	1.99822	DUF3575 domain-containing protein
Q8A8Q1	BT_1116	2.7145	3.31	PPC domain-containing protein
Q89Z34	BT_4543	2.54599	3.24113	Putative type I restriction enzyme specificity protein
Q8A174	BT_3792	2.47739	1.88394	alpha-1,6-mannanase
Q8A0W2	BT_3909	2.1813	1.63533	Unknown
Q8A2T3	BT_3222	2.146	1.39245	DUF4848 domain-containing protein
Q8A2T2	BT_3223	2.05685	3.09966	OMP_b-brl domain-containing protein
Q8A6W1	BT_1765	1.85376	2.45838	Levanase (2,6-beta-D-fructofuranosidase)
Q8A3A2	BT_3052	1.82297	3.1166	AraC family transcriptional regulator
Q8A8I7	BT_1180	1.70579	1.8163	Glycoside transferase family 4
Q8A0E0	BT_4081	1.69799	1.36892	SusC homolog
Q8A113	BT_3858	1.64563	1.41392	Alpha-1,2-mannosidase
Q8A9K1	BT_0814	1.60821	1.70922	BamA/TamA family outer membrane protein
Q8AB18	BT_0294	1.60238	1.35371	Carboxypeptidase regulatory-like domain-containing protein
Q8A5R5	BT_2173	1.38299	1.42681	SusD homolog
Q8A151	BT_3816	1.33909	1.3211	Penicillin-binding protein 2 (PBP-2)
Q8AA46	BT_0619	1.27055	1.6609	Ion-translocating oxidoreductase complex subunit D, rnfD
Q8A109	BT_3862	1.18718	1.70627	Endo-alpha-mannosidase

Table S4: Comparative Proteomics- Δ*dma1* Top 25 Most Downregulated Genes

Protein ID	Gene	Fold Change	-Log(P-value)	Proposed Function
Q8A6F7	BT_1927	-5.75443	4.17785	Unknown
Q8ABI4	BT_0126	-3.70228	1.44507	Six-hairpin glycosidase
Q8A4Y4	BT_2463	-3.65105	3.00365	RNA polymerase ECF-type sigma factor
Q89ZQ0	BT_4326	-3.53782	2.86951	ABC transporter ATP-binding protein
Q89ZP7	BT_4329	-2.97173	2.49205	BFN domain-containing protein
Q8A8X2	BT_1045	-2.64843	2.85322	Concanavalin A-like lectin/glucanase
Q8A7D7	BT_1587	-2.61663	1.4901	GCN5-related N-acetyltransferase
Q8AAE0	BT_0525	-2.32145	1.32336	LruC domain-containing protein
Q8A826	BT_1348	-2.17801	2.67435	CDP-abequose synthase
Q89ZP8	BT_4328	-2.167	3.63516	Ribosomal RNA small subunit methyltransferase E
Q89ZP9	BT_4327	-2.12513	5.58384	DUF4836 family protein
Q8A149	BT_3818	-1.95031	1.38383	Gliding motility lipoprotein GldH
Q89YQ4	BT_4677	-1.90211	2.01555	Beta-lactamase-inhibitor-like PepSY-like domain-containing protein
Q8A5G3	BT_2276	-1.88136	1.51383	AI-2E family transporter
Q8A551	BT_2391	-1.74464	3.18011	Hybrid Two-component system
Q8A6C7	BT_1957	-1.70454	1.4706	DUF4465 domain-containing protein
Q8A8X3	BT_1044	-1.68106	3.56162	Secreted endoglycosidase, GH family 18
Q8A4A5	BT_2698	-1.65411	1.42781	Unknown
Q8AAL2	BT_0452	-1.63773	1.32215	SusC homolog
Q89YP0	BT_4691	-1.59995	1.64528	Ribosomal RNA large subunit methyltransferase F,rlmF
Q8A8X4	BT_1043	-1.59626	3.77015	SusD homolog
Q8A6F8	BT_1926	-1.5911	1.87538	OmpA/MotB domain protein
Q8A5H2	BT_2267	-1.56716	1.5167	Site-specific integrase
Q8A2R4	BT_3241	-1.50727	1.30956	SusD homolog

Start Position	End Position	Sequence	Posterior Error Probability
153	164	EKEEVEPVEETK	1.62E-05
187	195	DKLHIPAEK	0.0033255
189	195	LHIPAEK	0.038234
259	279	QANQVVDMEHHQPISFGLSVR	3.29E-14
285	302	GFSVETGLTYTLLSSDAK	1.01E-36
314	322	LHYLGIPLK	6.66E-06
323	330	ANWNFLDK	0.0044146
323	331	ANWNFLDKK	2.04E-05
356	377	ETVKPLQFSVSGAVGAQFNATK	1.58E-09
378	401	RVGIYVEPGVAYFFDDGSDVQTIR	4.09E-08
379	401	VGIYVEPGVAYFFDDGSDVQTIR	5.89E-08
402	415	KENPFNFNIQAGIR	6.49E-12
403	415	ENPFNFNIQAGIR	2.13E-09

Table S5: Tryptic peptides of Dma1 identified in the OMV fraction.

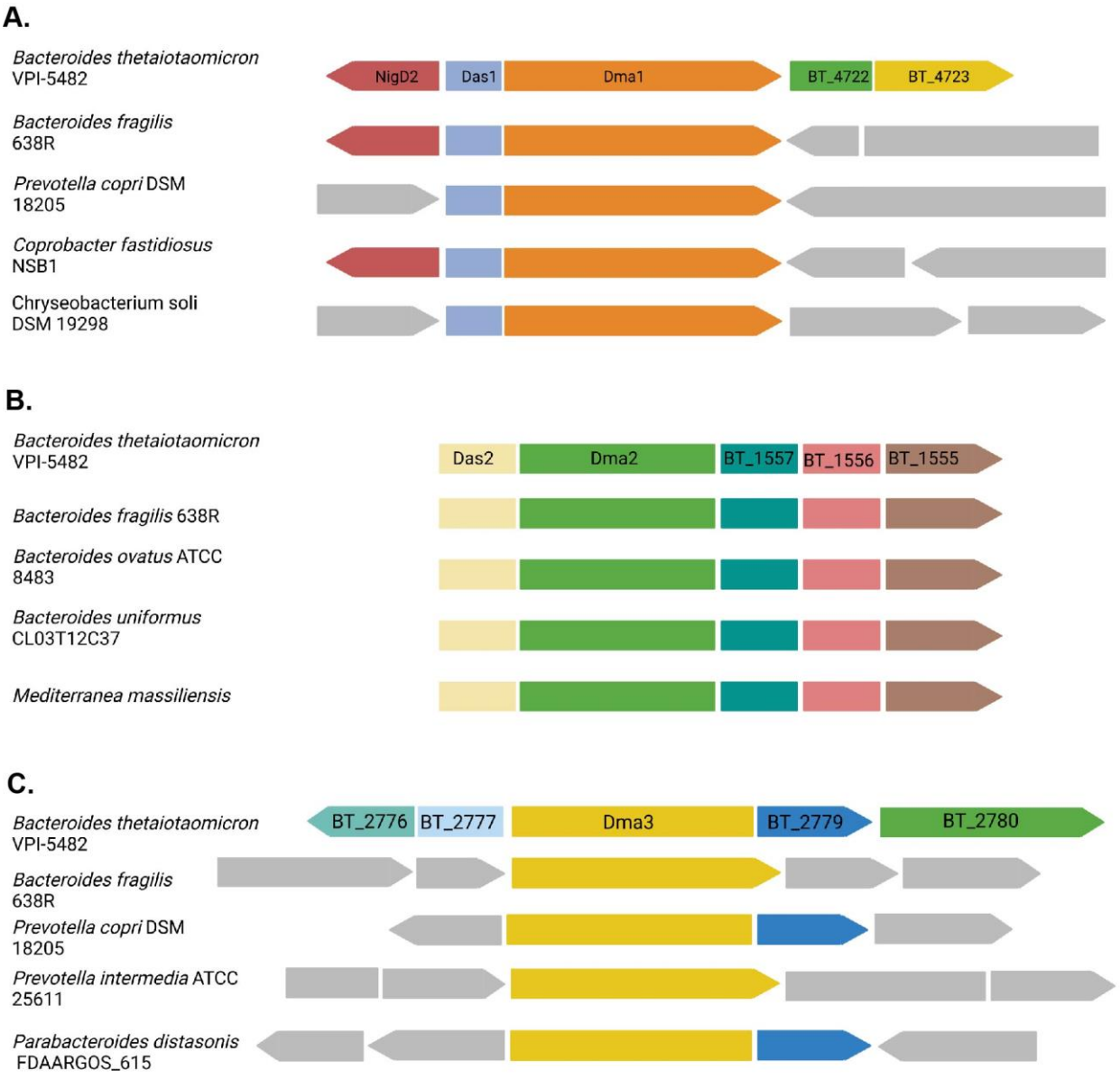

Figure S11: Schematic of gene synteny of *Bt* Dma1-3. Gene synteny for different Bacteroidota were compared to (A) Dma1 (BT_4721), (B) Dma2 (BT_1558), and (C) Dma3 (BT_2778) from Bt. Genes of the same color are conserved in different species, while those in grey differ.

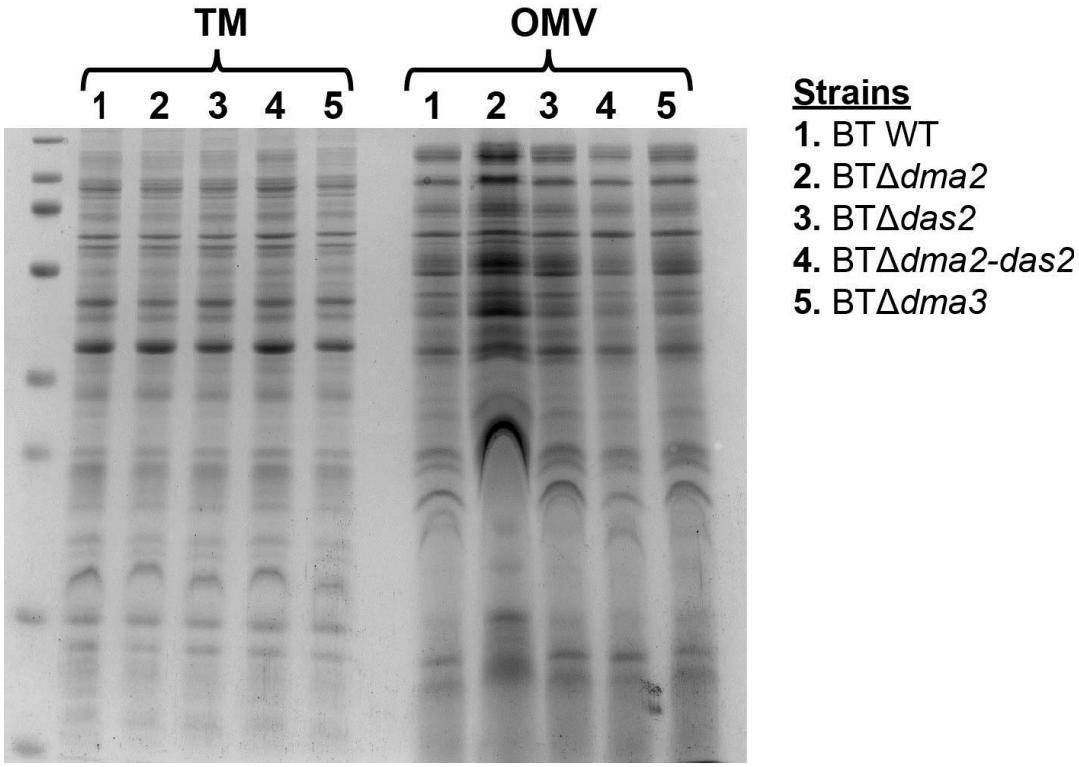

Figure S12: Δ*dma2* induces OMV biogenesis in a similar manner to Δ*dma1*. Coomassie Blue stain comparing protein profiles between WT, Δ*dma2*, Δ*das2*, Δ*dma2-das2*, and Δ*dma3*. This gel shows that mutation of *dma2* induces vesiculation, and this phenotype is dependent on its cognate sigma factor, Das2. Samples were normalized by OD_{600} values and run on 10% SDS-PAGE gel.